SUPPORTING INFORMATION

Explicit versus Implicit Solvent Modeling of Raman Optical Activity Spectra

Kathrin H. Hopmann, Kenneth Ruud, Magdalena Pecul, Andrzej Kudelski, Martin Dračínský, and Petr Bouř

Table S1. Relative electronic energies for QM-optimized single lactamide conformations

Conformer	B3LYP aug-cc-pVTZ Vacuum	B3LYP aug-cc-pVTZ IEFPCM	B3LYP aug-cc-pVTZ CPCM	B3LYP 6-311++G(d,p) CPCM	MP2 aug-cc-pVTZ CPCM
I	0.00	0.00	0.00	0.00	0.00
II	-0.29	0.61	0.61	0.47	0.72
III	-0.04	1.01	1.00	1.00	1.21
IV	-0.55	1.07	1.06	1.11	1.25

[a)] Energies are relative to Conformer **I** for each level of theory

Table S2. Relative Gibbs free energies (ΔG^{298K}) for QM-optimized single lactamide conformations

Conformer	B3LYP aug-cc-pVTZ Vacuum	B3LYP aug-cc-pVTZ IEFPCM	B3LYP aug-cc-pVTZ CPCM	B3LYP 6-311++G(d,p) CPCM
I	-0.10	0.00	0.00	0.00
II	-0.75	-0.02	0.02	0.01
III	0.00	1.05	1.04	1.17
IV	-0.72	0.98	0.99	1.24

[a)] Energies are relative to Conformer **I** for each level of theory

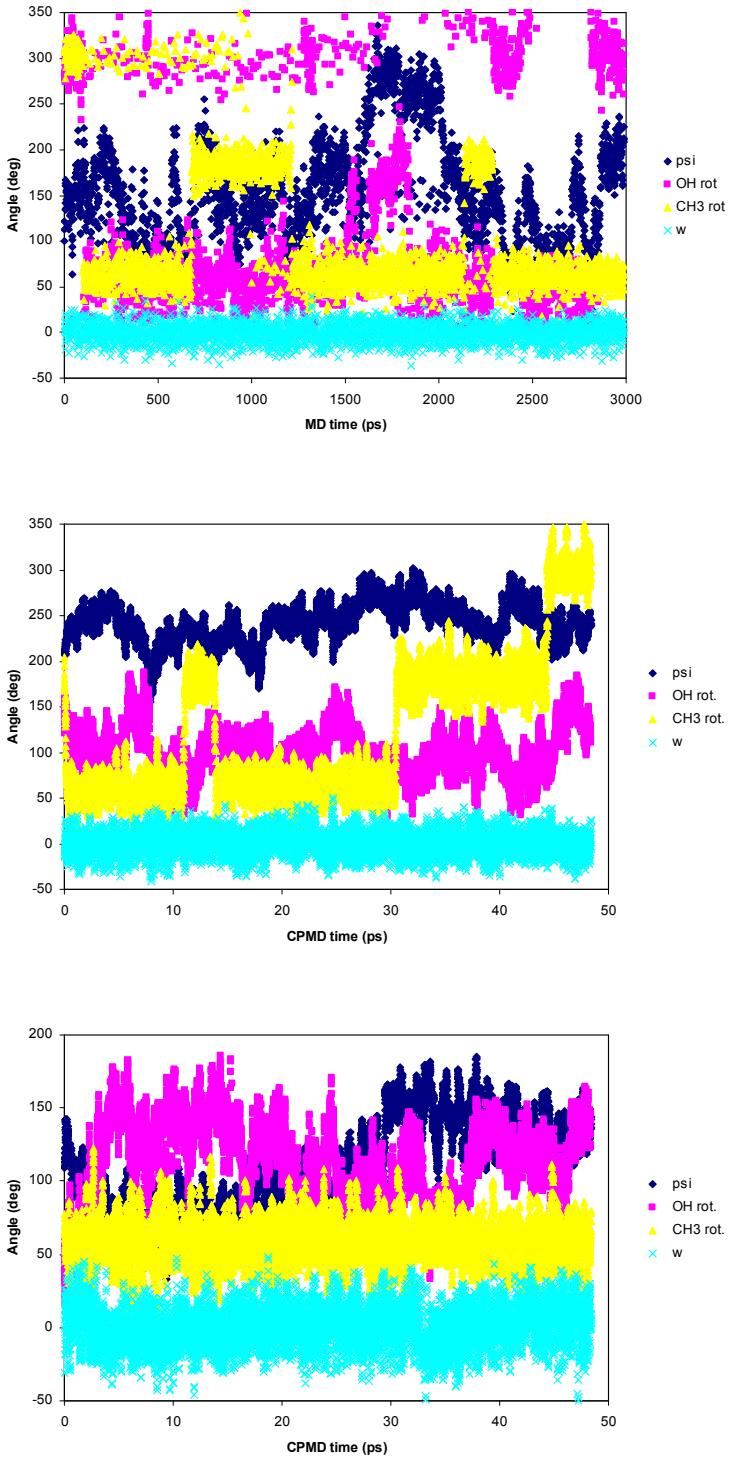

Figure S1. MD (top) and CPMD (run I-*anti,* middle, and II-*syn,* bottom) angle development for (R)-lactamide, angles $\psi = \angle(N,C,C,C)$, $\chi_{OH} = \angle(C(O),C,O,H)$, $\chi_{CH3} = \angle(C,C,C,H)$, and $\omega = \angle(H,N,C,C)$.

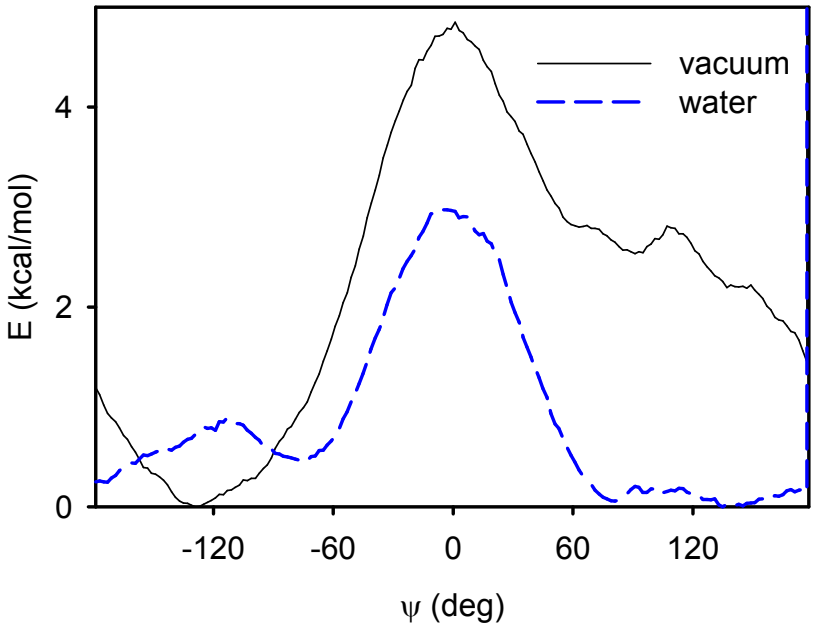

Figure S2. Potential of mean force obtained from the MD simulation (Amber99, 10 frames of 1000000 steops) for the ψ-angle of lactamide, in vacuum and for the hydrated molecule.

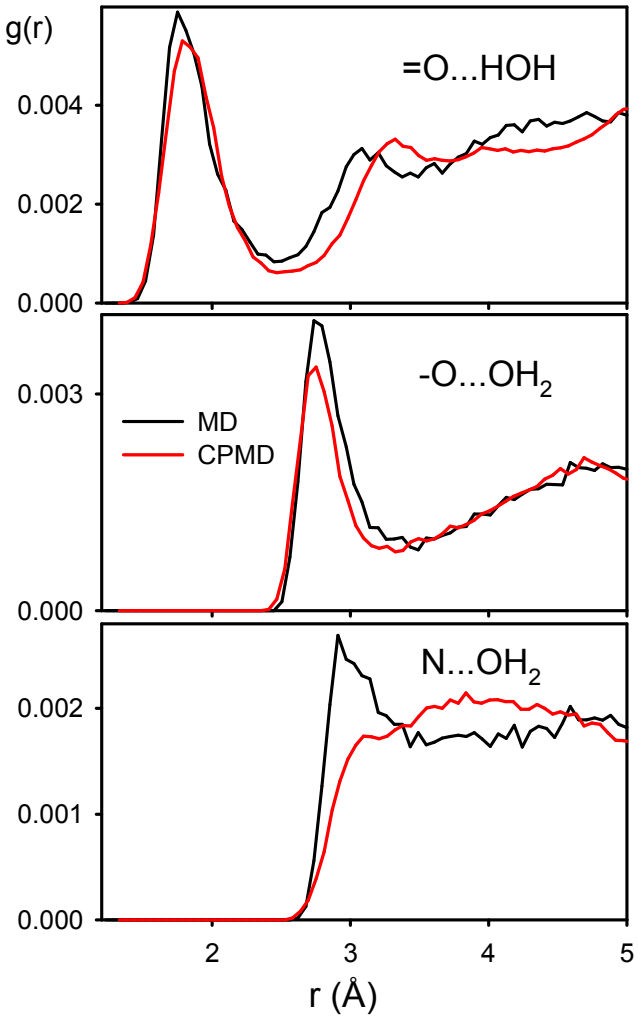

Figure S3. Radial distribution functions between the lactamide and water atoms, as calculated with the MD (Amber99 FF, 1 ns run, 18.56Å box) and CPMD (two 48-ps run average) dynamics.

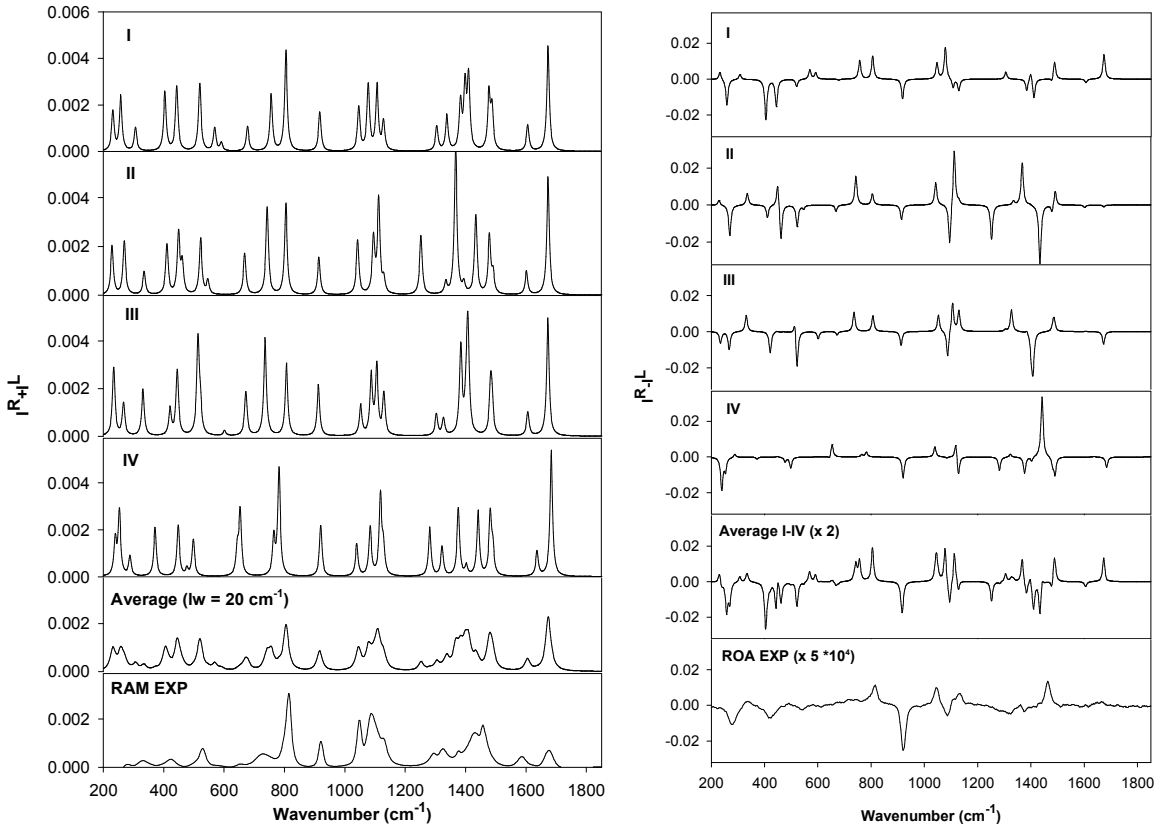

Figure S4. Computed (B3LYP/6-311++G(d,p)/CPCM) Raman (left) and ROA (right) spectra of individual (*R*)-lactamide conformers, averaged (Boltzmann distribution based on computed enthalpies, Table 1), and experimental spectra.

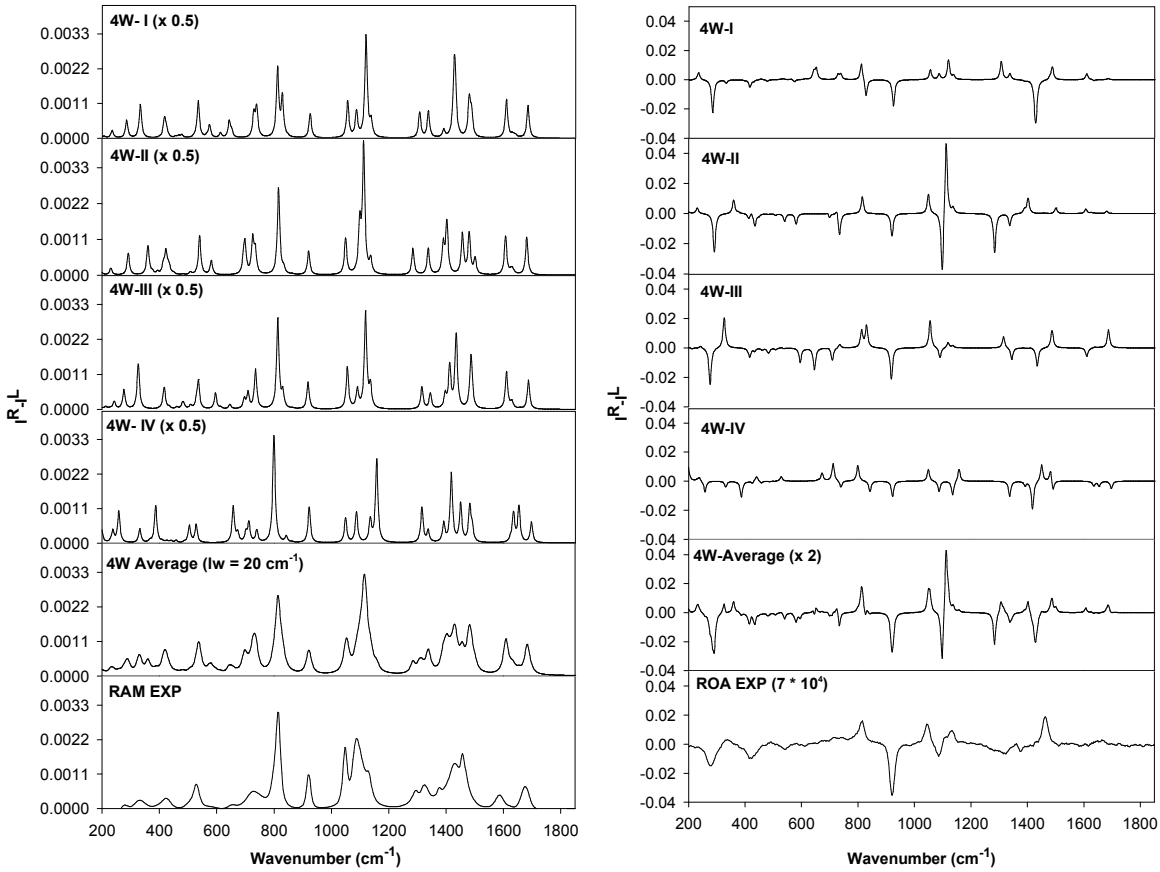

Figure S5. Computed (B3LYP/6-311++G(d,p)/CPCM) Raman (left) and ROA (right) spectra for the ad hoc hydrated conformers (4WI-IV) of lactamide, averaged (Boltzmann distribution based on computed enthalpies of solute, see text) and experimental spectra.

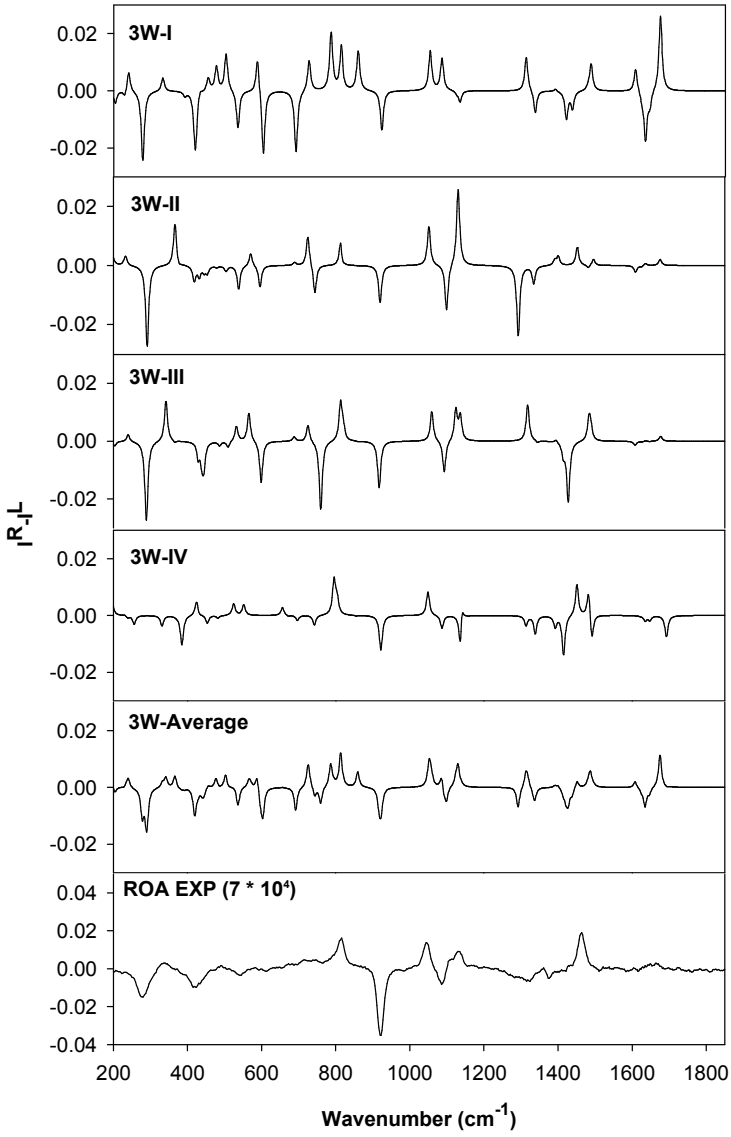

Figure S6. Computed ROA spectra for 3W conformers (I-IV) of (*R*)-lactamide (B3LYP/6-311++G(d,p)/CPCM), averaged spectrum (Boltzmann distribution based on computed enthalpies of solute, 39.6% I, 30.1% II, 24.5 % III and 5.8 % IV) and experimental spectrum.

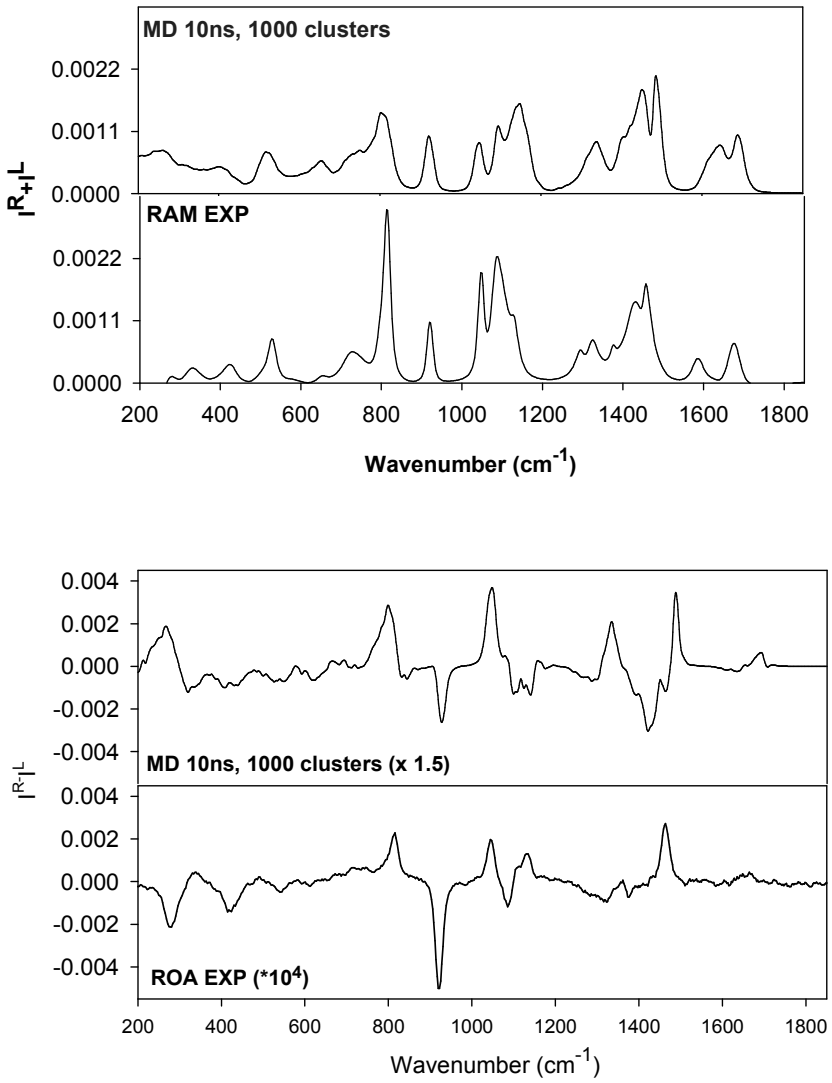

Figure S7. Raman (top) and ROA (bottom) spectrum computed from 1000 MD clusters (10 ns, clusters with 5 to 12 water molecules), and the experiment (EXP).

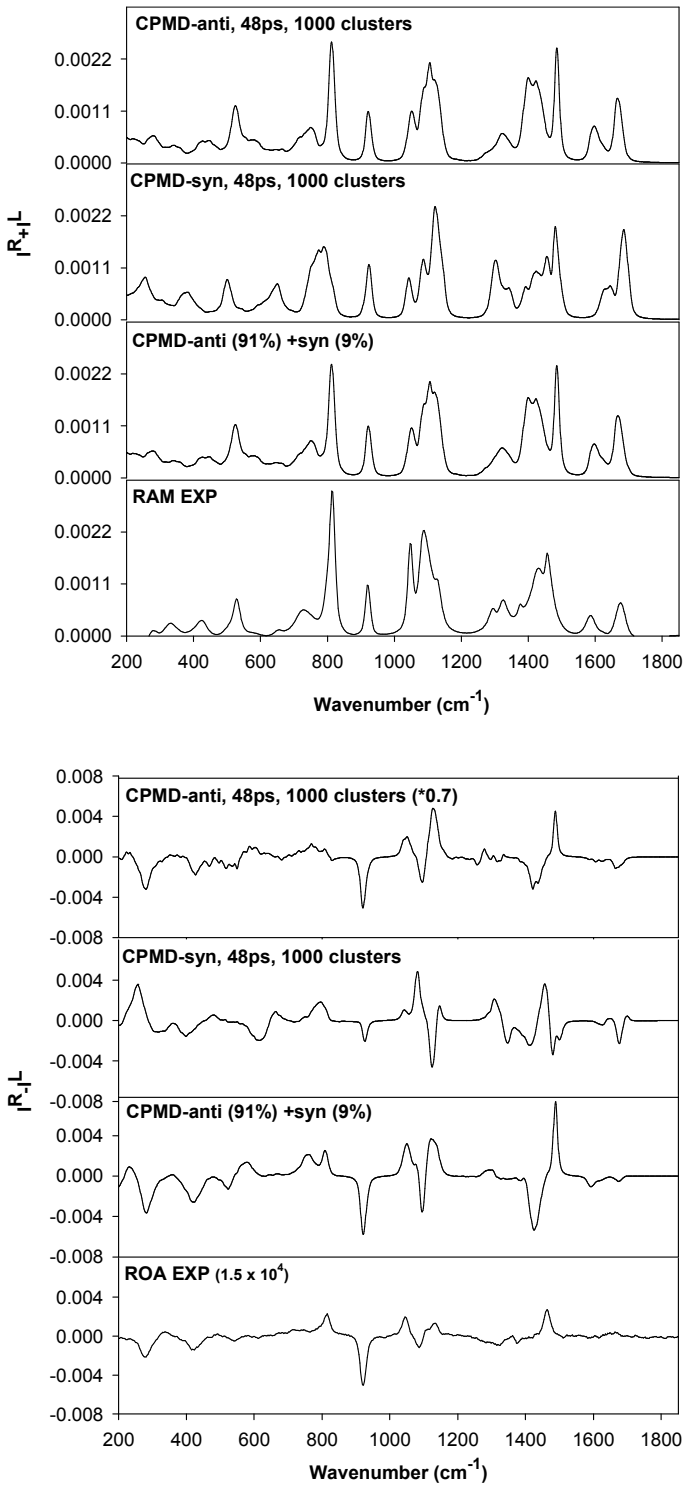

Figure S8. Computed Raman (top) and ROA (bottom) spectrum based on CPMD runs I (anti) and II (syn) of lactamide (each 48 ps, 1000 clusters, first hydrogen-bonded water shell), averaged spectrum and experimental spectrum.

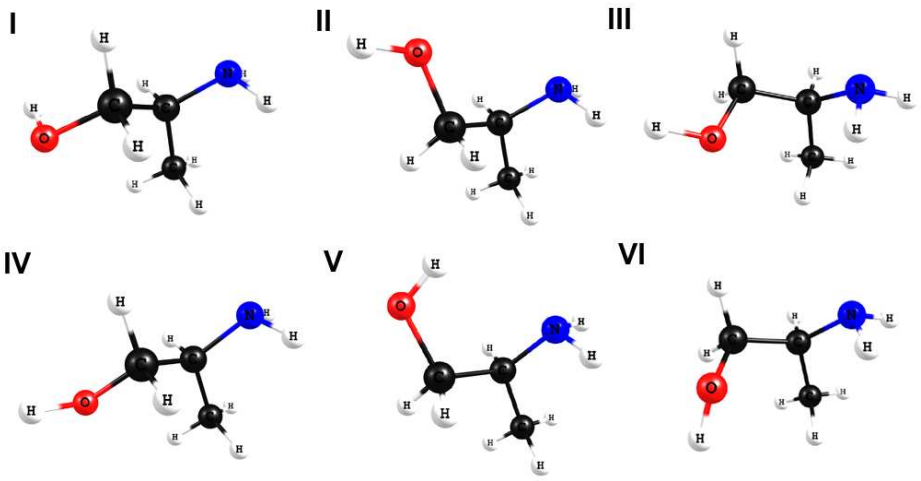

Figure S9. Optimized CPCM conformers I-VI of 2-aminopropanol. Boltzman distribution based on computed enthalpies is 63% for V, 13% I, 8% IV, 6% III, 6% VI and 4% II. For hydrated clusters (3 water molecules), the distribution is almost the same, 65% for V, 9% I, 7% IV, 7% III, 8% VI and 4% II.

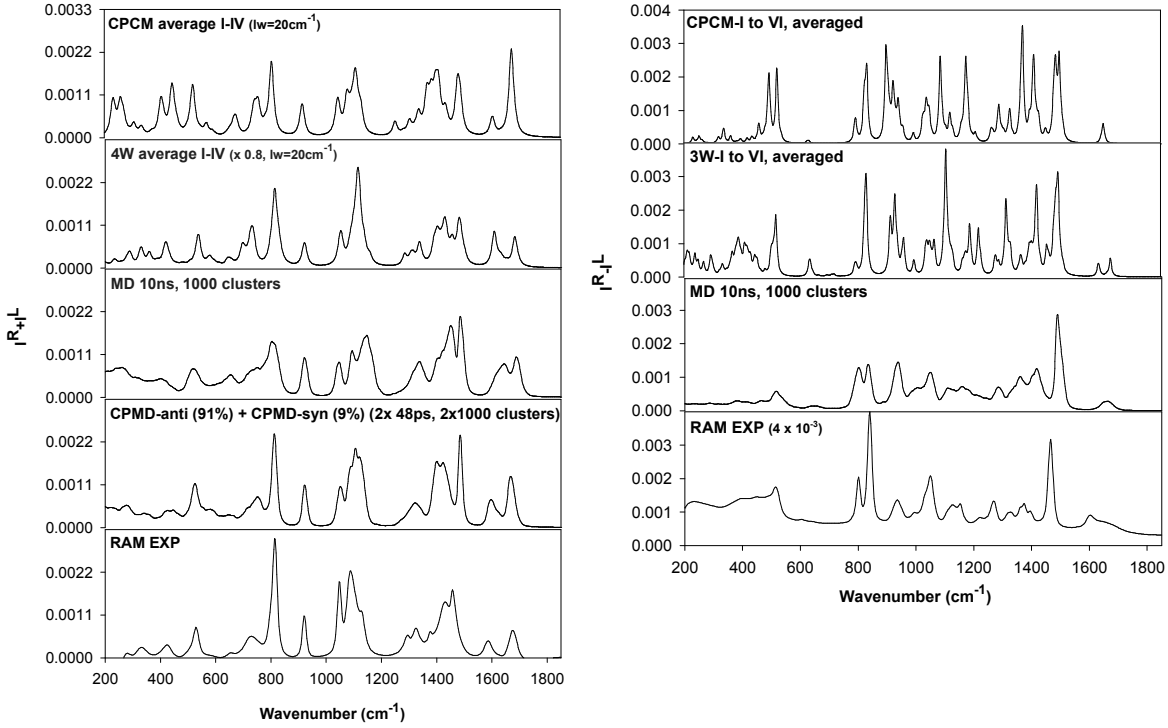

Figure S10. Comparison of computed (CPCM, 4W, MD, CPMD) and experimental Raman spectra for lactamide (left) and 2-aminopropanol (right).

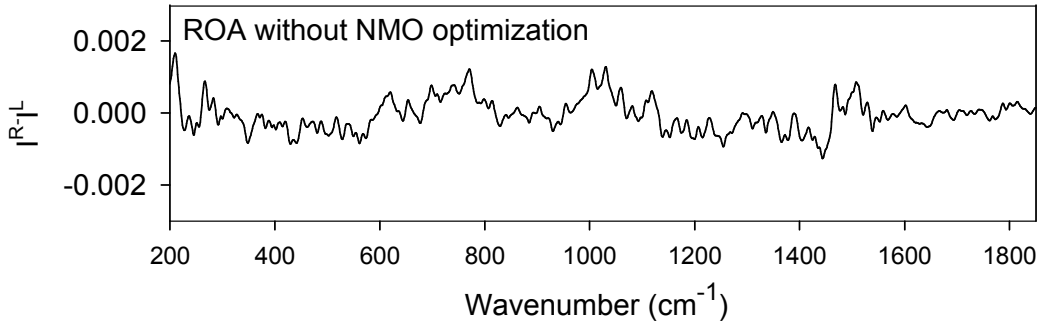

Figure S11. Computed ROA spectrum for lactamide without NMO optimization of MD clusters (100 MD clusters, 1 ns).

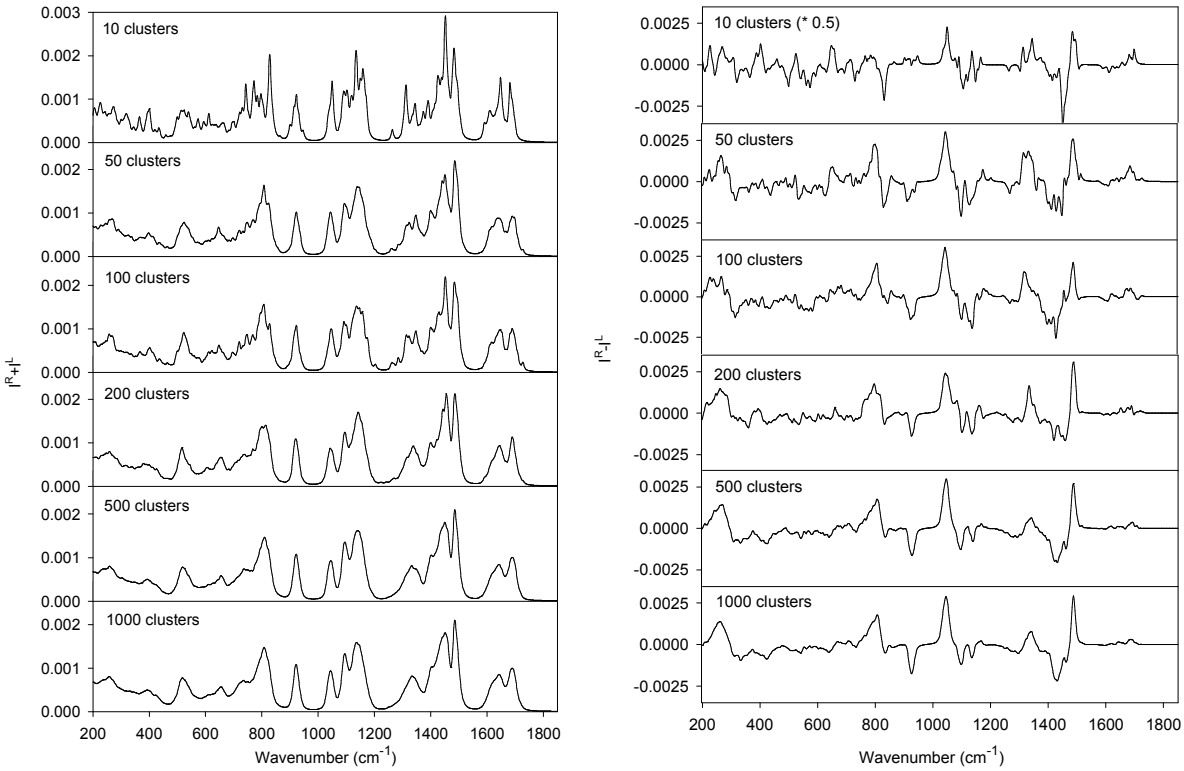

Figure S12. Computed Raman (left) and ROA (right) spectra based on 50 to 1000 MD clusters of lactamide (corresponding to 1 ns simulation, clusters including first hydrogen-bonded water shell).

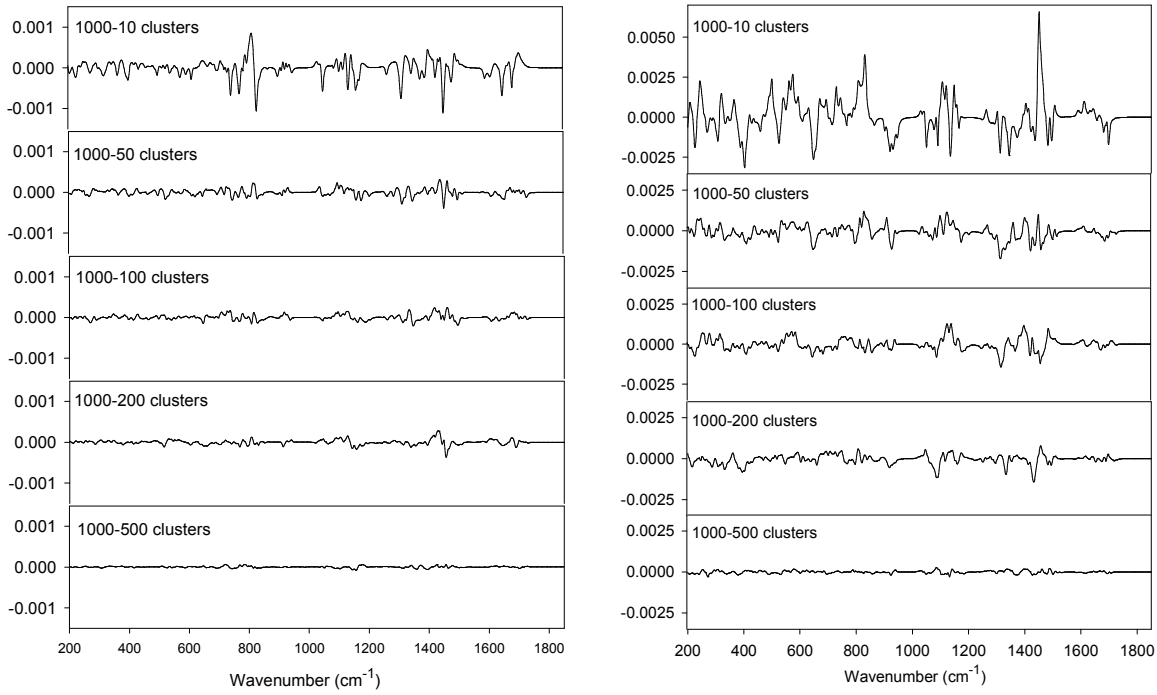

Figure S13. Difference between computed Raman (left) and ROA (right) spectrum based on 1000 MD snapshots (with first hydrogen-bonded water shell, spanning 1 ns) and spectra based on 10, 50, 100, 200 or 500 snapshots.

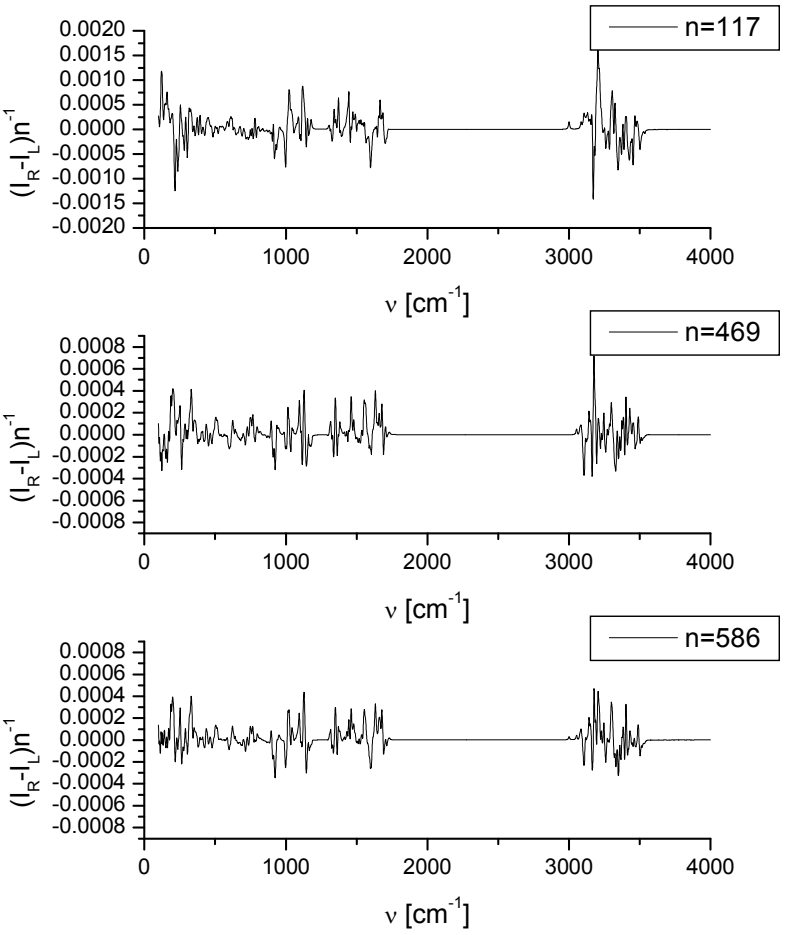

Figure S14. ROA spectra of glycine based on n MD snapshots.